

EXPERIMENTAL VERIFICATION OF DARHT AXIS 1 INJECTOR PIC SIMULATIONS*

A. F. Press[†], M. A. Jaworski, D. C. Moir, S. Szustkowski
 Los Alamos National Laboratory, Los Alamos, USA

Abstract

Validated particle in cell (PIC) simulations of the DARHT Axis 1 injector have the potential to reduce accelerator downtime, assist experimental data analysis and improve accelerator tunes. To realize these benefits, the simulations must be validated with experimental results. In this work, the particle in cell code Chicago is used to simulate the injector region of the dual-axis radiographic hydrodynamic test facility (DARHT) first axis. These simulations are validated against experiment using measured anode-cathode voltage, beam current at three positions, optical transition radiation and previously calculated emittance. Since all of these measurements contain some variation, the respective simulation parameters are varied to understand their effect. The resulting simulated beam current distributions can then be compared to the measured $2 \times \text{RMS}$ radius. This resulted in a reasonably well validated simulation model. Some inconsistency between simulated and measured results still exists, which future work will address.

EXPERIMENTAL AND SIMULATION SETUP

Figure 1 shows the DARHT Axis 1 injector geometry. Simulations are performed using the particle in cell code Chicago [1]. The anode magnet focuses the beam, while the bucking coil has the opposite polarization and is set to reduce the on-axis axial magnetic field to zero at the cathode face. The optical transition radiation (OTR) foil creates optical light proportional to the beam current density passing through it for a given beam energy. The foil is at a 50° angle, allowing the emitted light to be imaged using a gated CCD camera. The image is then corrected for angle and a background subtraction is performed. Figure 2 shows an example OTR image. An important factor in the OTR data is the width of the gate (10 ns, shown in Fig. 2) causing a small portion of the energy and current variation to be sampled. Only beam properties in the “flat-top” or steady state portion of the voltage and current pulse will be considered here. A range of beam profiles can be measured by changing the anode magnet field intensity. This results in a relationship between the anode magnet current and $2 \times \text{RMS}$ beam radius at a given axial position as shown in Fig. 3. A similar simulation geometry can be found in work performed by Plewa

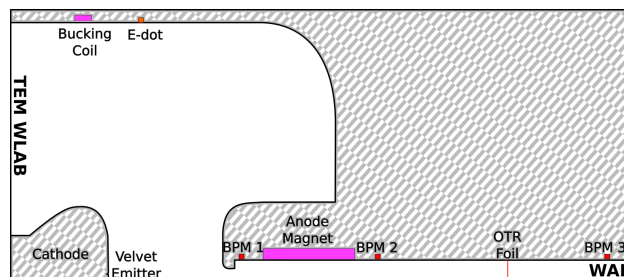


Figure 1: Geometry of the DARHT Axis 1 injector (not to scale). Far left vacuum boundary is a transverse electromagnetic launch and wave absorbing boundary (TEM WLAB). Far bottom right vacuum boundary is a wave absorbing boundary (WAB). The E-dot measures the cathode-anode voltage and was cross calibrated with permanent magnet spectrometer [4]. The anode-cathode gap is nominally 18 cm. BPM 1, 2 and 3 measure beam current at 24.5, 82.4 and 208.0 cm from the cathode face. The OTR measurement foil is located 163.0 cm from the cathode face. The velvet emitter is slightly recessed from the cathode face.

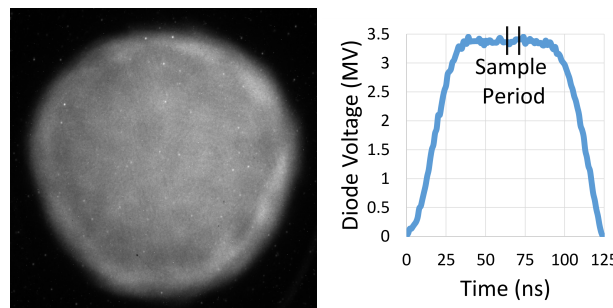


Figure 2: Left: OTR image taken 163 cm from the cathode face with an 186 A anode magnet current. Corrected for OTR foil angle. Right: Pulsed diode voltage showing flat-top and OTR sample period.

et al. [2], while detailed emitter region simulations can be found in work performed by Coleman *et al.*, [3].

SIMULATION VALIDATION

There are several free parameters which need to be constrained in the simulation:

1. **Input voltage** is adjusted until the anode-cathode (diode) gap voltage is equal to that measured by the E-dot.

* This work is supported by the US Department of Energy through the Los Alamos National Laboratory. Los Alamos National Laboratory is operated by Triad National Security, LLC, for the National Nuclear Security Administration of the U.S. Department of Energy (Contract No. 89233218CNA000001).

[†] alexpress@lanl.gov

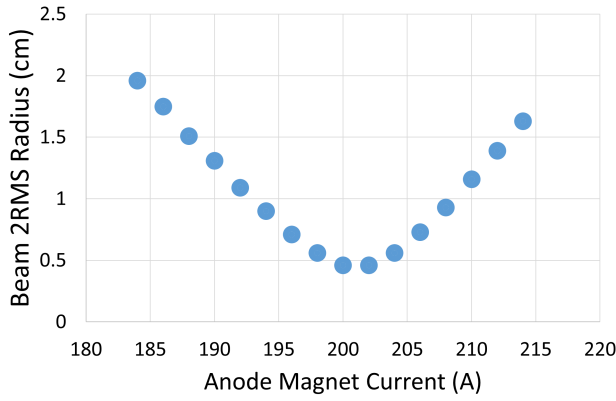


Figure 3: OTR measured 2*RMS beam radius at 163 cm from the cathode face as a function of anode magnet current.

- Beam current** is space charge limited and is controlled by the emission area for a given input voltage. The emission area is adjusted by increasing or decreasing the velvet emitter recess from the cathode shroud. As the depth is increased, the electric field is reduced at the emitter edges. This reduces the area of the emitter that reaches the breakdown threshold, reducing total current. The emitter depth is adjusted until the simulated and measured beam currents match.
- Emittance** has been calculated using OTR images and a fitting routine in the envelope code XTR [5]. The initial beam temperature is adjusted until beam emittance matches XTR calculated values.

Variation in Measured Quantities

Each measured quantity has some variation during the “flat top” portion of the pulse. Moir *et al.* [6] used a permanent magnet spectrometer to measure beam energy over a pulse. For a diode voltage near 3.34 MV, the RMS energy spread during a 60 ns portion of the pulse flattop was 0.43%.

Figure 4 shows three PIC simulated solenoid sweeps with roughly 0.5% changes in the diode voltage. The distribution of 2*RMS beam radii shifts to higher anode magnet currents as the diode voltage increases. This can be explained as an increase in anode magnet focal length, which is approximated by the thin lens formula [7]:

$$f = \frac{4\beta^2\gamma^2m^2c^2}{q^2 \int B^2 dz}, \quad (1)$$

where β and γ are the usual relativistic factors, m is the rest mass of an electron, c is the speed of light, q is the elementary charge and B is the on-axis axial magnetic field. Both β and γ increase with diode voltage, causing the increase in focal length.

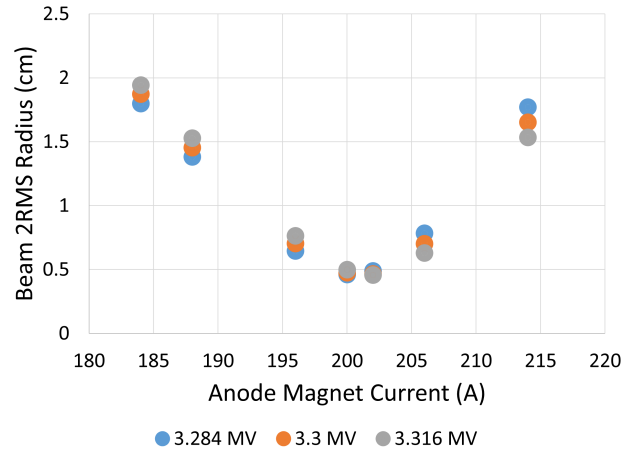


Figure 4: 2*RMS beam radius solenoid sweep for various diode voltages.

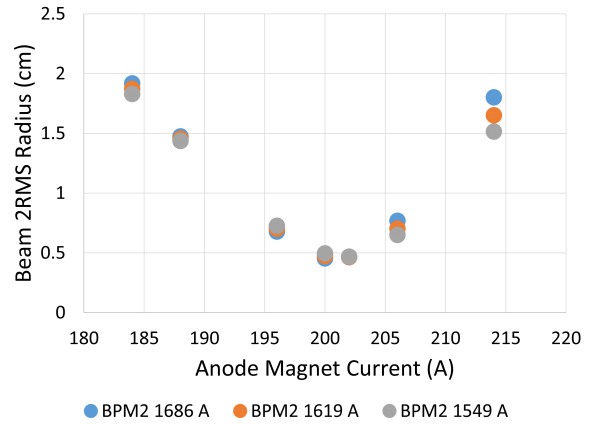


Figure 5: 2*RMS beam radius solenoid sweep for various beam currents.

An approximation to the relativistic 1D Child–Langmuir law gives the current (I) - voltage (V) relation [8]:

$$I \propto \frac{\left(\left(\frac{V(MV)}{0.511} + 1\right)^{2/3} - 1\right)^{3/2}}{(\sqrt{3} - 1)\left(\frac{V(MV)}{0.511} + 1\right)^{-0.392} + 1}. \quad (2)$$

Using this relation for a diode voltage of 3.34 MV, a 0.43% change results in a 0.54% change in beam current. A change in current of this magnitude is not obvious and so Figure 5 shows three PIC simulated solenoid sweeps with roughly 4% changes to the beam current. Since an increase in current comes from an increase in initial beam radius, and corresponds to an increased self electric field force, the beam will have a larger radius in the anode magnet region. Consequently the beam compress faster for a given anode magnet focal length, increasing the slope on the left hand side of Fig. 5. The higher compression causes a tighter pinch, leading to faster expansion and a larger slope on the right side of the figure.

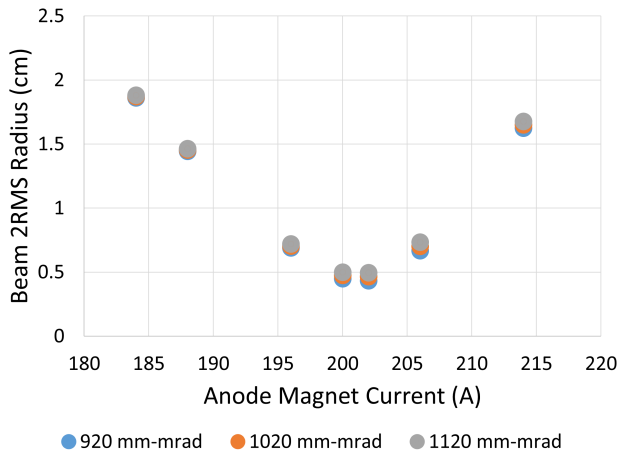


Figure 6: 2*RMS beam radius solenoid sweep for various initial emittance values.

Finally, the normalized emittance of a thermal emitter is given by [7]:

$$\epsilon_n = 2r_{\text{emit}} \sqrt{\frac{k_B T_e}{mc^2}}, \quad (3)$$

where r_{emit} is the radius of the emitting area, k_B is the Boltzmann constant and T_e is the electron temperature. For a 55 mm diameter emitter, the emittance is calculated to be $1200 \pm 10\%$ mm-mrad using a fitting routine in the XTR code. Generally the fitting routine calculates a 10% error in emittance due to the fit, other error sources are not included. Figure 6 shows three PIC simulated solenoid sweeps with roughly 10% changes in the normalized emittance, which was varied by changing the emitted electron temperature only. Changes can be seen in the 2*RMS minimum region, where a larger emittance produces a larger 2*RMS minimum. Using the trends shown in Figs. 4–6, a simulated solenoid sweep which reasonably matches the measured values can be found.

MATCHING MEASURED TO SIMULATED SOLENOID SWEEPS

Figure 7 shows the closest match between measured and simulated 2*RMS beam radius over a solenoid sweep. The input parameters are 3.3 MV, 1.69 kA and 1090 mm-mrad for the diode voltage, beam current and normalized emittance respectively. Both the diode voltage and normalized emittance are within reasonable values to those measured, however the current is larger than expected. Further, the 2*RMS radius values do not match for the highest anode magnet current simulated. Future work will address these discrepancies.

FUTURE WORK

To address discrepancies between measured and simulated data, comparisons between the full OTR measured and simulated radial profiles, or x-y transverse profiles will be made, rather than the less instructive 2*RMS values.

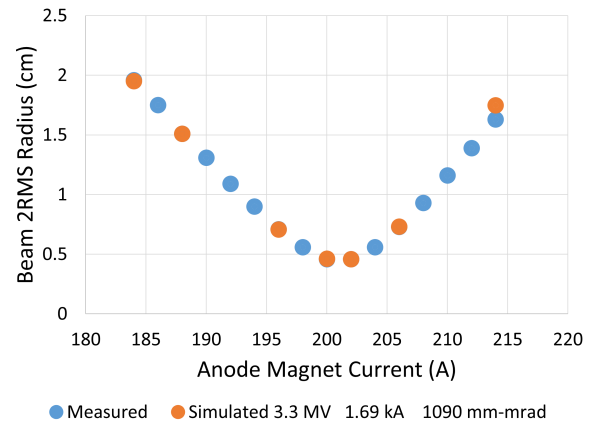


Figure 7: Best-matched measured (blue) and simulated (orange) 2*RMS beam radius solenoid sweep.

Work will also be performed to constrain the beam's initial phase space through experimental measurement using inverse Thomson scattering, a set of simulation to OTR measurement comparisons using a design of experiments or machine learning approach, or simulations which run the simulation backwards using the OTR data and an assumption for beam temperature.

REFERENCES

- [1] C. Thoma, D. Welch, R. Clark, D. Rose, and I. Golovkin, "Hybrid-pic modeling of laser-plasma interactions and hot electron generation in gold hohlraum walls," *Physics of Plasmas*, vol. 24, no. 6, p. 062707, 2017.
- [2] J. Plewa *et al.*, "High power electron diode for linear induction accelerator at a flash radiographic facility," *Physical Review Accelerators and Beams*, vol. 21, no. 7, p. 070401, 2018, doi: 10.1103/PhysRevAccelBeams.21.070401
- [3] J. E. Coleman, D. C. Moir, M. T. Crawford, D. R. Welch, and D. Offermann, "Temporal response of a surface flashover on a velvet cathode in a relativistic diode," *Physics of Plasmas*, vol. 22, no. 3, p. 033508, 2015, doi: 10.1063/1.4914851
- [4] T. J. Burris-Mog *et al.*, "Calibration of two compact permanent magnet spectrometers for high current electron linear induction accelerators," *Review of Scientific Instruments*, vol. 89, no. 7, p. 073303, 2018, doi: 10.1063/1.5029837
- [5] P. Allison, "Beam dynamics equations for XTR," Los Alamos National Lab., Los Alamos, NM, USA, Tech. Rep. LA-UR-01-6585, 2001.
- [6] D. C. Moir, T. Burris-Mog, N. D. Kallas, M. A. Jaworski, and B. T. McCuistian, "Optimization of DARHT axis I injector voltage," Los Alamos National Lab., Los Alamos, NM, USA, Tech. Rep. LA-UR-20-23236, 2020, doi: 10.2172/1648059
- [7] M. Reiser, *Theory and design of charged particle beams*, eng, 2nd. Wiley-VCH, 2008, doi: 10.1002/9783527622047
- [8] Y. Zhang *et al.*, "Simple solutions for relativistic generalizations of the child langmuir law and the langmuir blodgett law," *Physics of Plasmas*, vol. 16, no. 4, p. 044511, 2009, doi: 10.1063/1.3124135